AGU PUBLICATIONS

Geophysical Research Letters

RESEARCH LETTER
10.1002/2014GL059744

Key Points:
- Automatic delineation of bifurcation channels in a global river network map
- A new channel bifurcation flow scheme in a global hydrodynamic model
- Simulation with bifurcation flow shows reasonable agreement to observations

Correspondence to:
D. Yamazaki,
d-yamazaki@jamstec.go.jp

Citation:
Yamazaki, D., T. Sato, S. Kanae, Y. Hirabayashi, and P. D. Bates (2014), Regional flood dynamics in a bifurcating mega delta simulated in a global river model, *Geophys. Res. Lett.*, *41*, 3127–3135, doi:10.1002/2014GL059744.

Received 27 FEB 2014
Accepted 15 APR 2014
Accepted article online 21 APR 2014
Published online 14 MAY 2014

Regional flood dynamics in a bifurcating mega delta simulated in a global river model

Dai Yamazaki[1,2], Tomoko Sato[3], Shinjiro Kanae[4], Yukiko Hirabayashi[5], and Paul D. Bates[2]

[1]Department of Integrated Climate Change Projection Research, Japan Agency for Marine-Earth Science and Technology, Yokohama, Japan, [2]School of Geographical Sciences, University of Bristol, Bristol, UK, [3]Department of Mechanical and Environmental Informatics, Tokyo Institute of Technology, Tokyo, Japan, [4]Department of Civil Engineering, Tokyo Institute of Technology, Tokyo, Japan, [5]Institute of Engineering Innovation, University of Tokyo, Tokyo, Japan

Abstract In this paper we show the importance of bifurcation channels for flow in river mega deltas through the use of a new computational scheme implemented in the global hydrodynamic model, CaMa-Flood (Catchment-based Macro-scale Floodplain model). First, we developed a new river network map based on SRTM3 DEM (Shuttle Radar Topography Mission 3 arc-second Digital Elevation Model) and HydroSHEDS (hydrological data and maps based on shuttle elevation derivatives at multiple scales) which includes bifurcation channels. Next, we implemented a new bifurcation scheme in CaMa-Flood capable of routing flow along this network and used the model to simulate the Mekong River. We show that in the Mekong delta such channels route about 50% of total flow and that their representation is essential for realistic hydrodynamic simulations. A simulation without bifurcation channels was obviously unrealistic because no flow occurred between the mainstem and adjacent channels even when their water level difference was $>$6 m. The bifurcation channels are extracted from globally available data sets; thus, it is straightforward to expand the proposed scheme to global-scale studies.

1. Introduction

River mega deltas are one of the most vulnerable regions to flood hazard as a result of their very low and flat topography and susceptibility to river overflow and storm surge. Nearly 500 million people are estimated to live in mega delta regions globally [*Syvitski and Saito*, 2007], thereby a significant number of people are considered to be at risk of flooding. Flood risk in mega deltas may also increase in the future due to sea level rise, an intensification of the hydrological cycle associated with climate change [*Ericson et al.*, 2006; *Hirabayashi et al.*, 2013], land subsidence [*Syvitski et al.*, 2009], and population growth.

Modeling complex flow dynamics in mega deltas is essential for flood risk assessment, but this has not yet been achieved in global-scale (or even continental-scale) river models which are a fundamental tool for interbasin assessments of global hydrological changes [e.g., *Hirabayashi et al.*, 2013]. Global river models utilize river network maps in order to describe upstream-downstream relationships between grid cells [e.g., *Oki et al.*, 1999; *Decharme et al.*, 2008]. For about two decades, it has been assumed that each grid cell in a river network map has only one downstream direction [e.g., *Miller et al.*, 1994; *Yamazaki et al.*, 2009]. This assumption is true for most river networks, but it is not applicable to mega deltas due to their divergent channel system. Channel bifurcation can be represented in regional hydrodynamic models which explicitly solve two-dimensional flows in river channels and floodplains based on a high-resolution ($\leqq$1 km) digital elevation model (DEM) [e.g., *Bates and De Roo*, 2000; *Neal et al.*, 2012]; however, it is not straightforward to apply regional hydrodynamic models to simulations of one or multiple deltas due to the large spatial scale and significant amount of boundary data processing. Channel bifurcation can be represented in continental-scale vector river models [e.g., *Le et al.*, 2007], but required manual processing of a river network data restricts application of such models to multiple river basins. For such a task, continental- or global-scale hydrodynamic models which represent floodplain inundation as a subgrid physics are required.

In this study, we abandon the traditional assumption of one downstream direction in global river models in order to represent the bifurcation channel systems in mega deltas. We propose a fully automated algorithm to create a reasonable representation of bifurcation channels in a global river network map using subgrid topography information. A new flow scheme for bifurcation channels is then implemented in the catchment-based macroscale flood (CaMa-Flood) global hydrodynamic model [*Yamazaki et al.*, 2011] to

simulate the flow along bifurcated channel networks, and the impact of the bifurcation channels on the hydrodynamics of mega deltas is examined.

2. Method and Data

2.1. Experiment Setting

The Mekong River basin (E90–110, N5–35) was selected as a study area. The Mekong River is the largest river basin in the Southeast Asia (drainage area: 795,000 km^2, mean discharge: 16,000 m^3/s). The Mekong mega delta is highly populated and extensively farmed, and thus, flood hazard is a major concern of the local society. The spatial resolution of CaMa-Flood was set to 0.1°, and the simulation domain (90–110°E, 5–35°N) includes the entire basin of the Mekong (Figure 1d). Hydrodynamic simulations were executed with and without the channel bifurcation scheme in order to evaluate the impact of these channels on the hydrodynamics of the delta. The gridded runoff database by *Kim et al*. [2009] was used as input forcing to CaMa-Flood. The downstream boundary water level at the river mouths was set to 0 m (constant, equivalent to mean sea surface elevation); thus, ocean tides are not considered in this study. The simulation period was from 2001 to 2005 because of the availability of validation data sets.

2.2. Global River Model: CaMa-Flood

CaMa-Flood is a global-scale distributed river model, which is driven by runoff forcing from a land surface model and calculates river hydrodynamics (i.e., river discharge, water level, and inundated area). River basins are discretized into unit catchments (Figure 1b, black boundaries) which have subgrid river and floodplain topography parameters to represent floodplain inundation as a subgrid-scale process. River discharge is calculated by the local inertial equation [*Bates et al*., 2010; *Yamazaki et al*., 2013] between upstream and downstream unit catchments prescribed by a river network map (Figure 1a, blue lines). The local inertial equation explicitly represents backwater effect. According to *Bates et al*. [2010], the local inertial equation can be discretized and modified into

$$Q^{t+\Delta t} = \frac{Q^t + \Delta t\, gAS}{\left(1 + \frac{\Delta t\, gn^2|Q^t|}{h^{4/3}A}\right)}, \tag{1}$$

where $Q^{t+\Delta t}$ is the discharge between times t and $t+\Delta t$, Q^t is the discharge at the previous time step, A is the flow cross-sectional area (m^2), h is the flow depth [m], g is the gravitational acceleration (ms^{-2}), n is the Manning's friction coefficient ($m^{-1/3}$ s), and S is the water surface slope between the upstream and downstream unit catchments. The Manning's roughness coefficient for main river channels was set to 0.03 [*Chow*, 1959]. The calculation time step is automatically adjusted so as to satisfy the Courant-Friedrichs-Lewy condition [see *Bates et al*., 2010; *Yamazaki et al*., 2013].

The calculation chain at each time step is as follows: (step 1) water level and inundated area are diagnosed from water storage in each unit catchment, assuming the water surface elevations of river channel and floodplain areas are the same within a single unit catchment; (step 2) river discharge from each unit catchment to its downstream unit catchment along the river network map is calculated by the local inertial equation; (step 3) water storage at each unit catchment is updated by a mass conservation equation considering discharge input from the upstream unit catchment(s), discharge output to the downstream unit catchment, and local runoff input. For a more detailed description of CaMa-Flood, please refer to previous papers [*Yamazaki et al*., 2011, 2012a, 2013]. The new calculation method for the bifurcation channels flow is explained in section 2.3

The river network map and its subgrid topography parameters were extracted by applying the FLOW upscaling algorithm [*Yamazaki et al*., 2009] to the hydrological data and maps based on shuttle elevation derivatives at multiple scales (HydroSHEDS) flow direction map [*Lehner et al*., 2008; *Lehner and Grill*, 2013] and the Shuttle Radar Topography Mission 3 (SRTM3) DEM [*Farr et al*., 2007] at 3 arc sec (90 m) resolution. Errors and obstacles in the DEMs (e.g., vegetation canopy, contamination of elevations by levees and water surfaces, and random radar speckles) were removed to ensure consistent downhill flow along streamlines [*Yamazaki et al*., 2012b]. Pixels of the HydroSHEDS flow direction map are amalgamated to form unit catchments (Figure 1b, black boundary) by allocating one outlet pixel within each 0.1° grid box (Figure 1b, light blue dot). The river network map (Figure 1a, blue line) is extracted based on the upstream-downstream relationships

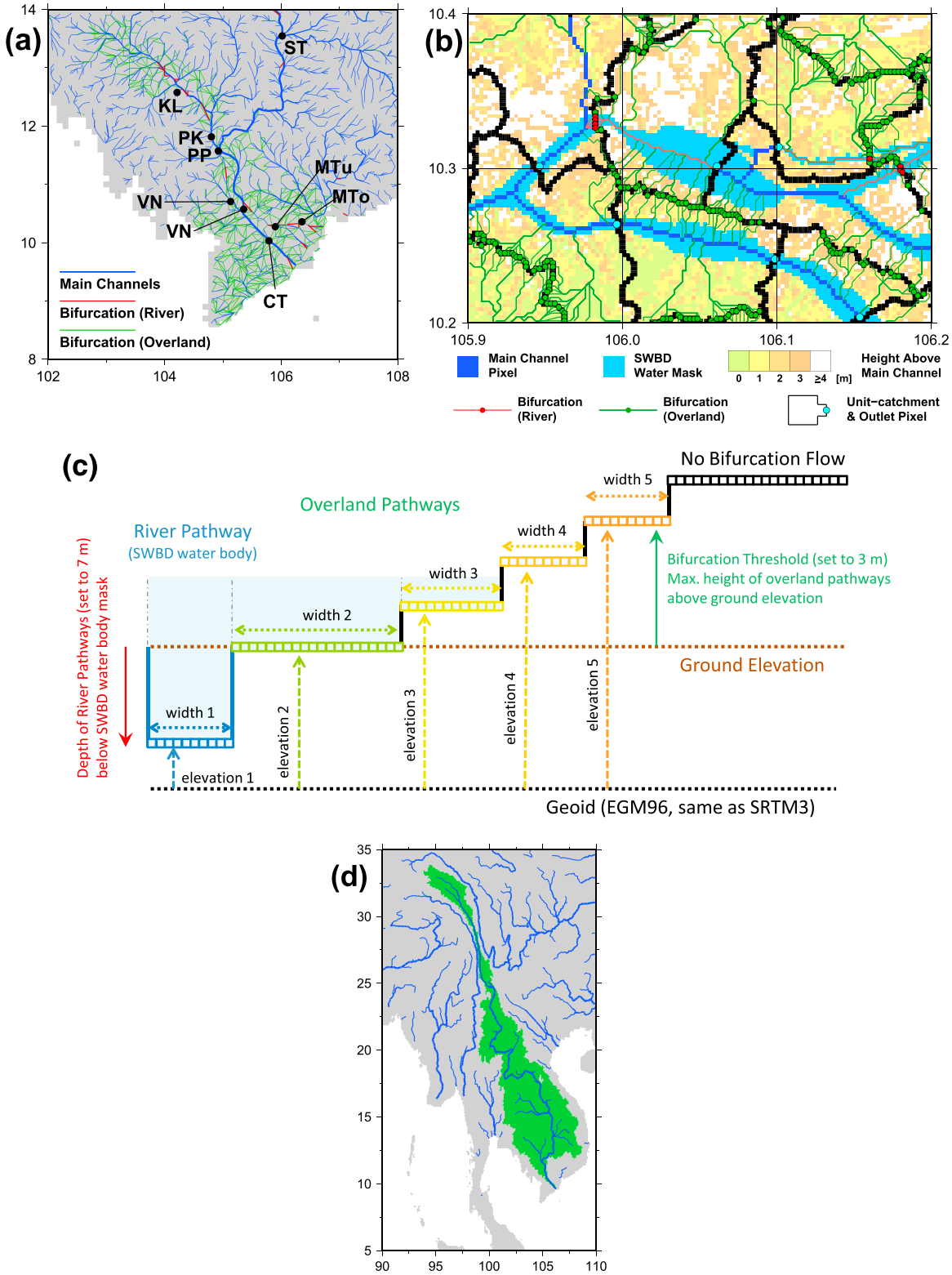

Figure 1. (a) River network map for the lower Mekong. Black dots represent gauging stations. ST: Stung Toreng, KL: Kompong Luong, PP: Phnom Penh Port, PK: Prek Kdam, CD: Chau Doc, VN: Vam Nao, CT: Can Tho, MTu: My Thuan, and MTo: My Tho. (b) Subgrid topography and bifurcation channels. (c) Schematic illustration of a bifurcation channel cross section after aggregating bifurcation pathways with the same elevations. Bifurcation channel's elevations and effective widths are indicated by the vectors "elevation 1–5" and "width 1–5." (d) The calculation domain.

between unit catchments. The subgrid topographic parameters (i.e., unit-catchment area, ground elevation, channel length, and floodplain elevation profile) are derived from the DEM and flow direction map (see *Yamazaki et al*. [2011] for detailed procedures).

2.3. Bifurcation Channel Scheme

Bifurcation channels are defined as channels connecting two unit catchments which do not have an upstream-downstream relationship in a river network map. The bifurcation channels are classified into "river pathways" (Figure 1a, red) and "overland pathways" (Figure 1a, green lines). River pathways represent bifurcated river channels with persistent bifurcation flow, while overland pathways represent flow routes in floodplains during flooding. We used the SRTM Water Body Data (SWBD) water mask [*NASA/NGA*, 2003] in order to detect the persistent bifurcated channels. Each bifurcation channel is represented by six parameters: upstream unit-catchment ID, downstream unit-catchment ID, bifurcation channel elevation, channel length, channel width, and roughness coefficient. Flow in a bifurcation channel occurs when the water surface elevation in either upstream or downstream unit catchment is higher than the bifurcation channel elevation.

Bifurcation channels are extracted by searching possible flow pathways crossing unit-catchment boundaries based on HydroSHEDS and SRTM3. Bifurcation flow must occur under the condition that when a pixel at a unit-catchment boundary (Figure 1b, black lines) is flooded and the flooded pixel has a higher water elevation than that in an adjacent pixel belonging to another unit catchment. The algorithm to define bifurcation channels works as follows. It first designates "potential bifurcation points" as being pixels which are at unit-catchment boundaries (Figure 1b, black lines) and which are not higher than the "bifurcation threshold height" (set to 3 m, green vector in Figure 1c) above the main channel of each unit catchment (Figure 1b, colored pixels). Note that the bifurcation threshold height was introduced to improve computational efficiency, and simulated hydrodynamics are not sensitive to the choice of threshold value when this is large enough. When the threshold value is large enough, bifurcation flows only occur in low elevation channels but not in high elevation channels. We confirmed by trial and error that a threshold of 3 m is sufficient in the case of the Mekong River. A potential bifurcation point is recognized as a valid bifurcation point (Figure 1b, red and green dots) if the ground elevation of an adjacent pixel belonging to another unit catchment is lower than the considered potential bifurcation point. The pathway along HydroSHEDS flow directions from each bifurcation point to the main channel pixels of its upstream and downstream unit catchments is defined as one bifurcation channel (Figure 1b, red and green lines). The side of the boundary with the higher (lower) elevation is treated as the upstream (downstream) unit catchment of the bifurcation channel. If both sides of the boundary are SWBD water body pixels, the bifurcation channel is treated as "river pathway" (Figure 1b, red dots). The length parameter of the bifurcation channel is given by calculating the flow length along each bifurcation channel (Figure 1b, red and green lines).

The width and elevation of the bifurcation channel are given as the size and elevation of the potential bifurcation pixel, respectively. If the bifurcation channel is classified as a "river pathway," the bifurcation channel's elevation is lowered using the river pathway depth parameter (set to 7 m by trial and error, red vector in Figure 1c) in order to represent channel bathymetry below the SRTM3 elevation. The river pathway depth is decided by trial and error. When there are multiple bifurcation channels connecting a pair of two unit catchments which have the same bifurcation channel's elevation, these bifurcation channels are aggregated into one "effective" bifurcation channel to improve computational efficiency (Figure 1c). The length and width parameters of the aggregated bifurcation channel are given by the mean and summation of bifurcation channels, respectively. Given that the vertical resolution of the SRTM3 elevation is 1 m, a pair of two unit catchments may have up to five bifurcation channels (one river pathway and four overland pathways with different elevations) when the bifurcation elevation threshold is set to 3 m (Figure 1c). The roughness coefficient of the bifurcation channel was set to 0.10 for "overland pathway" and 0.03 for "river pathway" following *Chow* [1959].

To route flow through this new global river network map, a new scheme for bifurcation channels flow was implemented into CaMa-Flood. Bifurcation channel flow is calculated after the river discharge calculation for main channels (between the calculation chain "step 2" and "step 3" in section 2.1). As for the main channel, bifurcation channel flow is calculated by the local inertial equation (equation (1)). The flow depth is given by the water level above the bifurcation channel elevation. The flow cross-sectional area is given by multiplying the flow depth and the bifurcation channel width. The water surface slope is calculated from the length and upstream and downstream water surface elevations of the bifurcation channel. After the discharge in main

channels and bifurcation channels has been calculated, the water storage in each unit catchment is updated using the mass balance equation.

2.4. Main Channel Parameters

The cross-section parameters of main channels (i.e., channel width and channel depth) cannot be extracted from the DEM and flow direction map. The channel width parameter is given from the Global Width Database for Large Rivers [*Yamazaki et al*., 2014], available at http://hydro.iis.u-tokyo.ac.jp/~yamadai/GWD-LR/. The channel depth parameter is estimated by the same empirical function of annual river discharge as in *Yamazaki et al*. [2012a, 2013]. However, the empirical function of annual river discharge underestimates channel depth in delta regions because annual river discharge is calculated without considering channel bifurcations. Therefore, channel depth parameters in the downstream part of a bifurcation channel are modified so that the same river bed elevation as the bifurcation channel's elevation is produced if the original river bed elevation is higher than the bifurcation channel's elevation.

2.5. Validation Data

We used in situ gauged discharges and water levels for validation. Nine gauges shown on Figure 1a were selected. The discharge at Prek Kdam was provided by *Inomata and Fukami* [2008], while other data were acquired from the Mekong River Commission. The discharge data at Prek Kdam are only available for 29 days during 2004 and 2005 (shown by grey dots in Figure 2), while the others are continuous daily observations.

3. Results

Simulated discharge and water level were compared against observations at the nine gauges (Figure 2; the locations of Stung Toreng and Kompong Luong are shown in Figure 1a). We first validated the applicability of the CaMa-Flood global hydrodynamic model to simulate flows in the upper part of the basin where bifurcation does not affect the result, by comparing the simulated and observed discharge at Stung Toreng (Figure 2, top right), which is the upstream boundary of the lower reach of the Mekong River. The annual mean discharge was underestimated by about 26% in the model simulation (11,020 m^3/s) compared to the observation (14,930 m^3/s). This difference is mostly due to the underestimation of low flow during dry seasons, caused by the underestimation of input runoff forcing. However, the annual mean peak discharge, which is important for mega delta hydrodynamics, was relatively well simulated (56,120 m^3/s in CaMa-Flood, 58,080 m^3/s in the observations). The correlation coefficient and the Nash efficiency between simulated and observed daily flows during 2001 through 2005 were 0.96 and 0.86, respectively. This analysis suggests that CaMa-Flood is capable of simulating discharge inflows to the mega delta. Note that there was no significant difference in simulated discharges between the experiments with and without bifurcation at Stung Toreng.

We then analyzed the difference between simulations with and without bifurcation channels in the mega delta region (Vam Nao, Chau Doc, Can Tho, My Thuan, and My Tho). Vam Nao and Can Tho are located on the main channel of the original HydroSHEDS river network (the upper Tien River and the lower Hau River), while My Thuan and My Tho are located on a secondary channel bifurcated from the mainstem (the lower Tien River and My Tho River, respectively). Chau Doc is located on the upstream Hau River which bifurcates from the Mekong mainstem at downstream of Phnom Penh and merges again to the mainstem (the lower Hau River) at downstream of Vam Nao. The delineated river network map with bifurcation channels well captures the divergent channel system of the Mekong delta (see the middle map of Figure 2). Because the gauged discharge and water level are affected by the ocean tide cycle, a 30 day moving average (black lines) is used for the comparison. The discharge and water level are largely overestimated in the mainstem (Vam Nao and Can Tho) when channel bifurcations are not represented (blue lines), while the simulation with bifurcation channels (red lines) shows a better fit to the gauged discharge and water level. In the secondary channels of the delta (My Thuan and My Tho), discharge and water level stay around zero in the simulation without the bifurcation scheme. The seasonal variations of discharge and water level in diverted channels are only simulated when the channel bifurcation scheme is used. The upper Hau River (where Chau Doc is located) is disconnected in the original HydroSHEDS river network. The simulation without bifurcation channel shows unrealistic negative discharge at Chau Doc in the high water season because of backward flow from the mainstem.

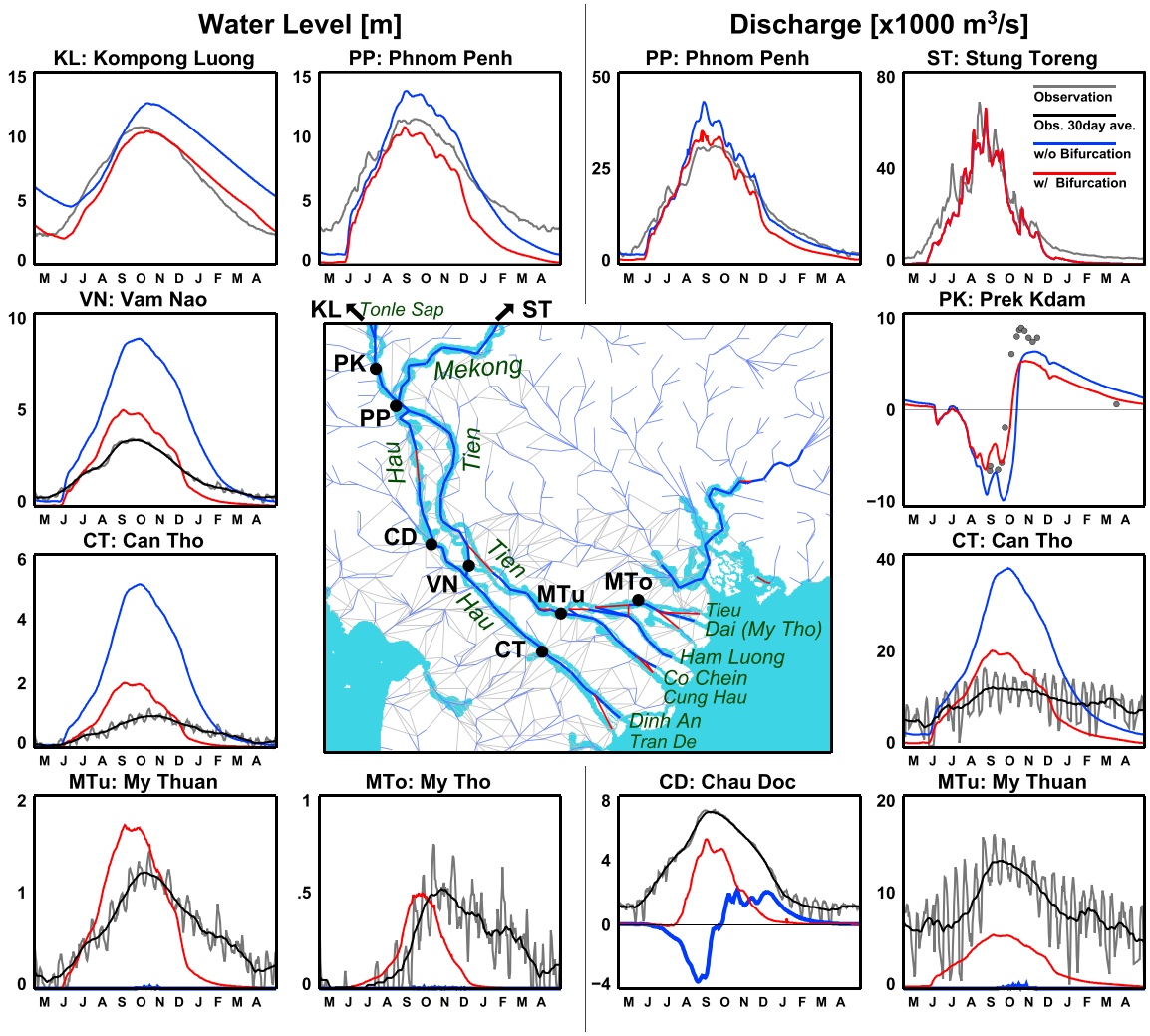

Figure 2. (left six panels) Water level and (right six panels) discharge at gauging stations from May 2001 to April 2002 (except for Prek Kdam which is from May 2004 to April 2005). Note that vertical axis has a different scale in a different panel. The map in the middle shows the gauge locations and the model's channel network (main channels: blue; river bifurcation: red; overland bifurcation: grey). River names are shown by dark green.

We found that bifurcation channel flow also affects the hydrodynamics in the region located upstream of the mega delta (Phnom Penh, Kompong Luong, and Prek Kdam). Given that river basin topography upstream of mega deltas is typically very flat, water level changes in the mega delta can potentially affect the hydrodynamics of surrounding regions as a result of backwater effects. The simulated maximum water level at Kompong Luong (in Tonle Sap Lake) and Phnom Penh (top of the Mekong delta) decreased by 1.76 m and 2.63 m, respectively, when bifurcation channels were considered. The error in mean water surface elevation between the simulation and observations decreased both in Kompong Luong and Phnom Penh (from +1.18 m to −0.58 m and from +1.89 m to −0.74 m, respectively). The backward flow at Prek Kdam caused by the reversal of water levels (from the Mekong mainstem to Tonle Sap Lake) was overestimated in the simulation without bifurcation channels because simulated water level was too high at Phnom Penh. The simulated backward flow showed better agreement to the observation when bifurcation channels were considered (RMSE of backward flow between the simulation and observation decreased from 3850 m^3/s to 1760 m^3/s). The simulated water levels at Phnom Penn are lower than the observation probably due to the underestimation of upstream inflow.

The simulated annual mean discharges in 2001 in the lower Mekong River are shown in Figure 3a. The simulation with bifurcation channels (Figure 3a, left) shows that many channels in the mega delta region

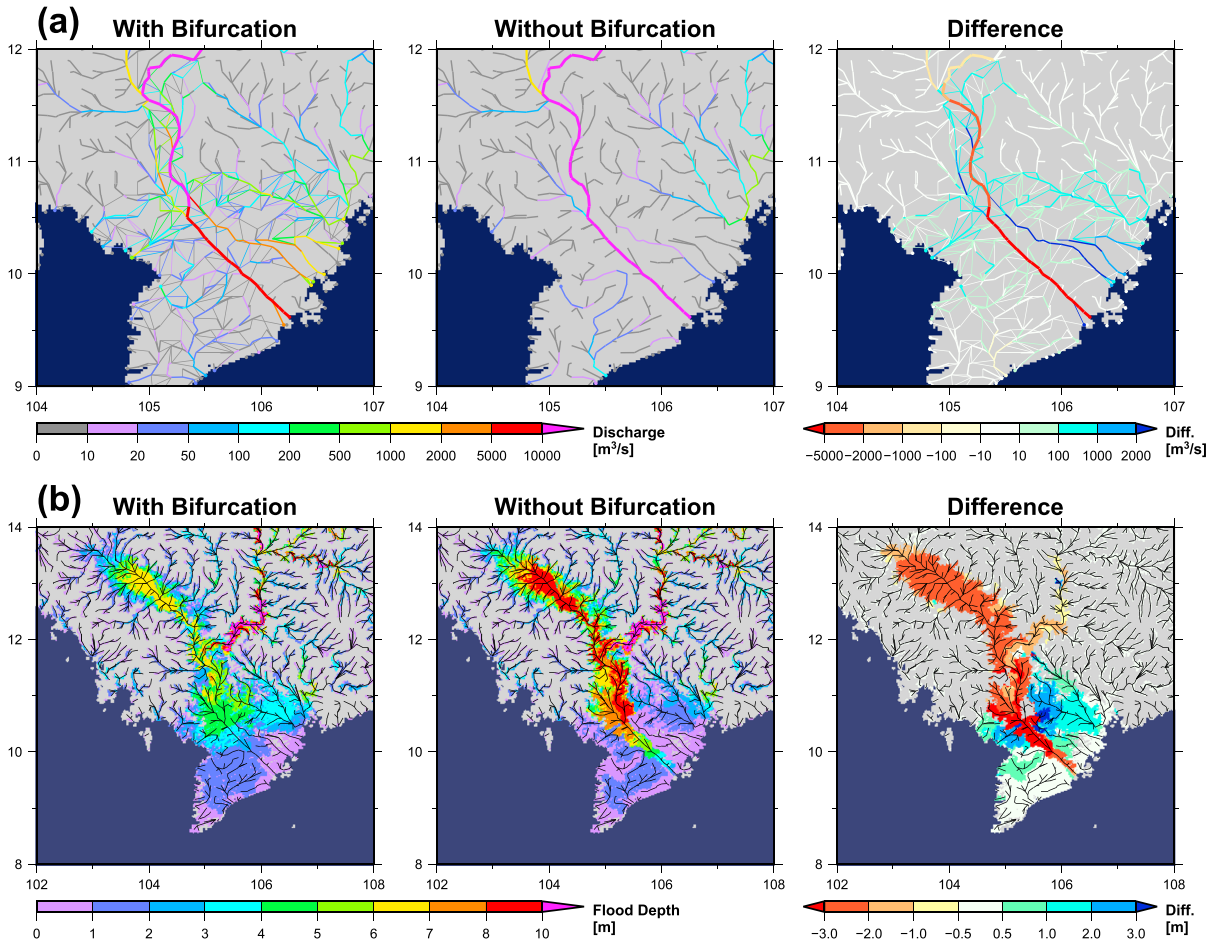

Figure 3. (a) Annual mean discharge in 2001. (b) Annual maximum flood depth in 2001.

have annual mean discharge of more than 100 m^3/s. Some bifurcation channels representing river pathways have an annual mean discharge larger than 1000 m^3/s. As expected, there are almost no flows in secondary channels bifurcated from the mainstem within the mega delta region in the simulation without bifurcation channels (Figure 3a, middle). This is because many channels in the mega delta regions are treated as independent river basins in the original river network map and interbasin flow does not occur without the bifurcation channel scheme. Thus, the discharge in the mega delta region is underestimated when bifurcation channels are not represented. The difference between the two simulations (Figure 3a, right) shows the annual mean discharge of the delta mainstem decreased from 15,900 m^3/s to 8,100 m^3/s when the bifurcation channel scheme is used. About 4800 m^3/s (30%) of annual mean discharge is diverted from the mainstem to the second largest channel in the mega delta, while the rest (3000 m^3/s) flows via overland pathways. It suggests that about 50% of the mainstem discharge is transferred to surrounding bifurcation channels in the mega delta region.

The maximum flood depth in 2001 is shown in Figure 3b. The simulation with bifurcation channels (Figure 3b, left) shows a smooth flood depth distribution in the mega delta region, while large differences in flood depths between the mainstem and other regions were found in the simulation without bifurcation channels (Figure 3b, middle). The difference between the two simulations (Figure 3b, right) suggests that water levels in mainstem decrease by 3 m or more when channel bifurcations are considered. The flood depth increase in the delta region caused by the water input from the mainstem via bifurcation channels is more than 3 m. The traditional assumption in global river models of only one downstream direction per grid cell is not applicable for mega deltas because it is obviously unrealistic that no flow occurs even when the water level difference is larger than 6 m between adjacent channels.

4. Conclusion

In this study, an algorithm to allocate bifurcation channels onto a global river network map is introduced to simulate complex flow dynamics in mega deltas. The bifurcation channels are automatically extracted from topography information in the HydroSHEDS flow direction map and the SRTM3 DEM. A new channel bifurcation flow scheme was implemented into the CaMa-Flood global river model to enable flow along this new river network map to be simulated. The impact of bifurcation channels on mega delta hydrodynamics was analyzed for the Mekong River basin by executing hydrodynamic simulations with and without the channel bifurcation scheme. The water level of the mainstem was overestimated in the simulation without bifurcation channels because no flow occurs from the mainstem to surrounding channels in the mega delta. Because the water level difference between the main channel and adjacent channels was unrealistically large ($>$6 m) in the simulation without bifurcation channels, the traditional assumption in global river models of only one downstream direction is obviously not applicable to mega deltas. About 50% of water was found to be transferred from the mainstem to surrounding bifurcation channels, suggesting that bifurcation channels play an important role in regulating the hydrodynamics of both mega deltas themselves and also the wider river basin as a result of backwater effects.

Two bifurcation channel parameters (the bifurcation channel depth and the bifurcation threshold height) are determined by trial and error in this study, thus calibration of these parameters may be required when the model is applied to other river basins. The bifurcation channel depth was set 7 m in the Mekong River, but the optimal depth parameter may be different in other river basins. Though the bifurcation threshold height does not affect simulation results when the threshold value is large enough, it should not be too large for keeping high computational efficiency. Note that the bifurcation threshold height is generally decided by the magnitude of flood wave heights. Given that the flood wave heights of the Mekong River is one of the largest in the world (about 7 m), the threshold value in this study (3 m) is considered to be acceptable for most river basins.

Uncertainties remain in the hydrodynamic simulations with bifurcation channels. The main channel depth was estimated by an empirical equation, which may not capture well the spatial variability of channel bathymetry due to local geology and climate. Because the empirical equation is not applicable to secondary channels bifurcated from the mainstem, uncertainty of channel bathymetry is larger in delta regions compared to the upstream catchment. Small bifurcation channels (such as artificial canals) are classified as overland pathways because they are not covered by the SWBD water mask. This may lead to the underestimation of flow in such channels because channel bathymetry is not considered in overland pathways. Reformation of channel network (e.g., switching of main channels in a delta), which may be important in long time scale simulations, is not represented in the current modeling framework. Despite the above uncertainties, the channel bifurcation scheme brought a significant improvement in the hydrodynamic simulation of mega deltas by a global river model and allows us to quantify, for the first time, the importance of such channels for mega delta hydrodynamics. Though some topographic parameters need to be calibrated, the channel bifurcation scheme proposed in this study only utilizes globally available databases, and thus, the application to other river mega deltas is straightforward.

Acknowledgments

The authors appreciate the Mekong River Commission for providing the gauge data used for the validation. The first author was supported by "JSPS Postdoctoral Fellowship for Research Abroad" from Japan Society for Promotion of Science (JSPS). This work was partially supported by "JSPS Grant-in-Aid for Scientific Research (ID: 23226012)." The CaMa-Flood global hydrodynamic model and associated data used in this study can be shared for research purposes. Please contact the corresponding author (Dai Yamazaki) to access to the model and data.

The Editor thanks Cédric David and an anonymous reviewer for their assistance in evaluating this paper.

References

Bates, P. D., and A. P. De Roo (2000), A simple raster-based model for flood inundation simulation, *J. Hydrol.*, *236*, 54–77, doi:10.1016/S0022-1694(00)00278-X.

Bates, P. D., M. S. Horritt, and T. J. Fewtrell (2010), A simple inertial formulation of the shallow water equations for efficient two-dimensional flood inundation modeling, *J. Hydrol.*, *387*, 33–45, doi:10.1016/j.jhydrol.2010.03.027.

Chow, V. T. (1959), *Open-Channel Hydraulics*, 680 pp., McGraw-Hill, New York.

Decharme, B., H. Douville, C. Prigent, F. Papa, and F. Aires (2008), A new river scheme for global climate applications: Off-line evaluation over South America, *J. Geophys. Res.*, *113*, D11110, doi:10.1029/2007JD009376.

Ericson, J. P., C. J. Vörösmarty, S. L. Dingman, L. G. Ward, and M. Meybeck (2006), Effective sea-level rise and deltas: Causes of change and human dimension implications, *Global Planet. Change*, *50*(1), 63–82.

Farr, T. G., et al. (2007), The Shuttle Radar Topography Mission, *Rev. Geophys.*, *45*, RG2004, doi:10.1029/2005RG000183.

Hirabayashi, Y., R. Mahendran, S. Koirala, L. Konoshima, D. Yamazaki, S. Watanabe, H. Kim, and S. Kanae (2013), Global flood risk under climate change, *Nat. Clim. Change*, *3*, 816–821, doi:10.1038/NCLIMATE1911.

Inomata, H., and K. Fukami (2008), Restoration of historical hydrological data of Tonle Sap Lake and surrounding areas, *Hydrol. Processes*, *22*(9), 1337–1350.

Kim, H., P. J.-F. Yeh, T. Oki, and S. Kanae (2009), Role of rivers in the seasonal variations of terrestrial water storage over global basins, *Geophys. Res. Lett.*, *36*, L17402, doi:10.1029/2009GL039006.

Le, T. V. H., N. H. Nguyen, E. Wolanski, T. C. Tran, and S. Haruyama (2007), The combined impact on the flooding in Vietnam's Mekong River delta of local man-made structures, sea level rise, and dams upstream in the river catchment, *Estuarine Coastal Shelf Sci.*, *71*, 110–116, doi:10.1016/j.ecss.2006.08.21.

Lehner, B., K. Verdin, and A. Jarvis (2008), New global hydrography derived from spaceborne elevation data, *Eos Trans. AGU*, *89*(10), 93–94, doi:10.1029/2008EO100001.

Lehner, B., and G. Grill (2013), Global river hydrography and network routing: baseline data and new approaches to study the world's large river systems, *Hydrol. Proc.*, *27*, 2171–2186, doi:10.1002/hyp.9740.

Miller, J. R., G. L. Russell, and G. Caliri (1994), Continental-scale river flow in climate models, *J. Clim.*, *7*, 914–928.

NASA/NGA (2003), SRTM Water Body Data Product Specific Guidance, Version 2.0. [Available at http://dds.cr.usgs.gov/srtm/version2_1/SWBD/SWBD_Documentation/.]

Neal, J., G. J.-P. Schumann, and P. D. Bates (2012), A simple model for simulating river hydraulics and floodplain inundation over large and data sparse areas, *Water Resour. Res.*, *48*, W11506, doi:10.1029/2012WR012514.

Oki, T., T. Nishimura, and P. Dirmeyer (1999), Assessment of annual runoff from land surface models using Total Runoff Integrating Pathways (TRIP), *J. Meteorol. Soc. Jpn.*, *77*(1B), 235–255.

Syvitski, J. P., and Y. Saito (2007), Morphodynamics of deltas under the influence of humans, *Global Planet. Change*, *57*, 261–282.

Syvitski, J. P., et al. (2009), Sinking deltas due to human activities, *Nat. Geosci.*, *2*(10), 681–686.

Yamazaki, D., T. Oki, and S. Kanae (2009), Deriving a global river network map and its sub-grid topographic characteristics from a fine-resolution flow direction map, *Hydrol. Earth Syst. Sci.*, *13*, 2241–2251, doi:10.5194/hess-13-2241-2009.

Yamazaki, D., S. Kanae, H. Kim, and T. Oki (2011), A physically-based description of floodplain inundation dynamics in a global river routing model, *Water Resour. Res.*, *47*, W04501, doi:10.1029/2010WR009726.

Yamazaki, D., H. Lee, D. E. Alsdorf, E. Dutra, H. Kim, S. Kanae, and T. Oki (2012a), Analysis of the water level dynamics simulated by a global river model: A case study in the Amazon River, *Water Resour. Res.*, *48*, W09508, doi:10.1029/2012WR011869.

Yamazaki, D., C. Baugh, P. D. Bates, S. Kanae, D. E. Alsdorf, and T. Oki (2012b), Adjustment of a spaceborne DEM for use in floodplain hydrodynamic modeling, *J. Hydrol.*, *436-437*, 81–91, doi:10.1016/j.jhydrol.2012.02.045.

Yamazaki, D., G. A. M. de Almeida, and P. D. Bates (2013), Improving computational efficiency in global river models by implementing the local inertial flow equation and a vector-based river network map, *Water Resour. Res.*, *49*, 7221–7235, doi:10.1002/wrcr.20552.

Yamazaki, D., F. O'Loughlin, M. A. Trigg, Z. F. Miller, T. M. Pavelsky, and P. D. Bates (2014), Development of the global width database for large rivers, *Water Resour. Res.*, *50*, doi:10.1002/2013WR014664.